https://doi.org/10.20965/jaciii.2018.p0076

Paper:

Power Curve Based-Fuzzy Wind Speed Estimation in Wind Energy Conversion Systems

Agus Naba and Ahmad Nadhir

Study Program of Instrumentation, Department of Physics, Faculty of Mathematics and Natural Sciences, University of Brawijaya
Jl. Veteran, Malang, East Java 65145, Indonesia
E-mail: {anaba, anadhir}@ub.ac.id

[Received December 26, 2016; accepted October 11, 2017]

Availability of wind speed information is of great importance for maximization of wind energy extraction in wind energy conversion systems. The wind speed is commonly obtained from a direct measurement employing a number of anemometers installed surrounding the wind turbine. In this paper a sensorless fuzzy wind speed estimator is proposed. The estimator is easy to build without any training or optimization. It works based on the fuzzy logic principles heuristically inferred from the typical wind turbine power curve. The wind speed estimation using the proposed estimator was simulated during the operation of a squirrel-cage induction generator-based wind energy conversion system. The performance of the proposed estimator was verified by the well estimated wind speed obtained under the wind speed variation.

Keywords: sensorless wind speed estimation, fuzzy logic principles, wind power, wind energy conversion system, wind turbines

1. Introduction

One of the most attractive solutions to energy shortage problems is a variable-speed Wind Energy Conversion System (WECS). Operating the variable speed WECS at optimum turbine rotor speed enables maximum extraction of wind energy at all wind speed irrespective of the type of generator used [1–6]. Optimum rotor speed is proportional to wind speed. The problem is that the wind speed information is not readily available. The wind speed and direction are also unpredictable from time to time and from location to location, adding more difficulty in operating the wind turbine at optimum speed.

An anemometer is commonly employed to measure wind speed. Such a direct measurement of the wind speed has the drawback that a number of anemometers are often required and need to be installed properly surrounding the wind turbine to obtain adequate wind speed information [2]. In addition, it is difficult to measure the wind speed exactly at the center of the wind turbine rotor and the measurement is not reliable when turbulence, shadowing, and aerodynamics interference occur [7–9]. On the contrary, indirect measurement methods of the wind speed are of attractive perspective technically and economically for WECS designs, particularly, of small and medium size.

Several methods for the wind speed estimation in WECS have been proposed. In [2, 3, 7, 10–12] the neural network based wind speed estimation methods are proposed in the MPPT control scheme. The control goal is to drive the turbine rotor as close as possible to the speed reference which is proportional to the wind speed estimate. Assuming accurate wind speed information, the MPPT control scheme is applied to maximize the wind energy extraction. Other methods [13–15] employ a fuzzy model to map the measured generator power and the turbine rotor speed into the reference maximum power. The mapping implicitly estimates the wind speed since the reference maximum power can be directly represented in term of the wind speed. Those methods [2, 3, 7, 10–15] need to train the neural network/fuzzy estimators. Despite obtaining good neural network/fuzzy estimator, the training process is usually costly and time-consuming, requiring good or ideal training data, while the trained estimators might be only applicable to certain conditions within the training data context used.

Indeed the fuzzy logic approach can be a very powerful tool for dealing with nonlinear input-output mapping provided that expert knowledge in terms of fuzzy rules *if-then* is available. It allows us to build fuzzy mapping with less or even no training. This advantage does not belong to any other mapping technique. In addition, given well defined fuzzy rules the fuzzy mapping would be more generally applicable in that it is not limited to the certain ranges of training data. In the previous research [13–15] the fuzzy mapping was designed without introducing any fuzzy expert rule. It was simply considered as a black box without any unique benefit over other mapping techniques.

In this paper a sensorless method for estimating wind speed using a fuzzy wind speed estimator (FWSE) is presented. FWSE works based on fuzzy rules simply inferred from a typical power curve of the wind turbine. The power curve represents the behavior of the wind turbine in terms of extracted power, rotor speed, and wind speed. It can be considered to be the most appropriate source of knowledge for inferring effective fuzzy rules that relate the wind speed with the rotor speed and the extracted

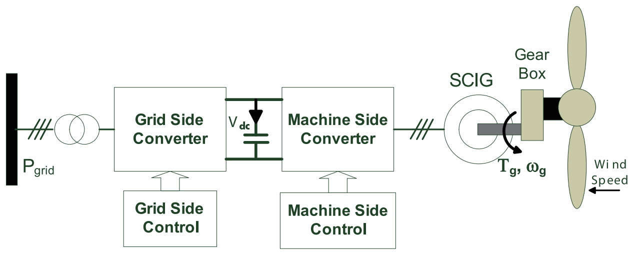

Fig. 1. Variable-speed SCIG-based WECS.

power. Since the typical power curve remains the same for most wind turbines, the inferred fuzzy rules would be generally applicable to most wind turbines.

The main contribution of the proposed approach is the ease of building FWSE without any training or optimization, yet capable of at least giving comparable performance with other wind speed estimation methods. In addition, the wind speed estimation based on the fuzzy rules simply inferred from the wind turbine power curve has never been attempted by any other research, except by Naba [16]. The work in this paper extends the preliminary work reported in [16] with more elaboration on the performance of the proposed wind speed estimation method.

2. Wind Energy Conversion System

The WECS model used in this paper is illustrated in **Fig. 1**. Its Simulink model is freely available in [17] and allows us to modify as necessary. It is of a horizontal-axis and variable-speed type and equipped with a squirrel-cage induction generator (SCIG). The SCIG-based WECS is considered as adequate for the discussion in this paper since the typical power curve of WECS equipped with other type of generator remains the same.

The wind turbine extracts wind energy from the swept area of the blades. Under the machine side control and the grid side control, the electrical energy resulting from the generator is converted by the machine side converter and the grid side converter into the voltage appropriate for the power grid system. The wind turbine extracts wind power according to [18]:

$$P = 0.5\pi\rho C_p(\lambda,\beta)R^2v^3 \quad \text{. . . . .} \quad (1)$$

where ρ is the air density, R is the turbine radius, v is the wind speed, $C_p(\lambda,\beta)$ is the power coefficient of the range of 25–45%, λ is the tip speed ratio (TSR), and β is the pitch angle. TSR is defined by

$$\lambda = \frac{\omega_r R}{v} \quad \text{. . . . .} \quad (2)$$

where ω_r is the turbine rotor speed.

The dynamic model of the wind turbine is given by

$$\frac{d\omega_r}{dt} = \frac{1}{J}(T_t - T_g - F\omega_r) \quad \text{. . . . .} \quad (3)$$

where J is the system inertia, F is the viscous friction coefficient, T_t is the torque resulting by the turbine, and T_g is the load torque due to the generator torque. The turbine rotor speed ω_r is transmitted to the generator through the gearbox with a certain multiplier, resulting in the larger generator speed ω_g.

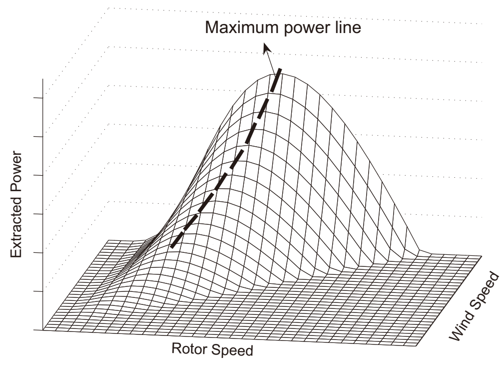

Fig. 2. Power curve.

In case of a fixed pitch angle, the extracted wind power varies non-linearly with the rotor speed and the wind speed as illustrated in **Fig. 2**. The maximum power points on the power curve for different wind speeds are shown by a maximum power line. They take place at the optimum rotor speed ω_{opt}, corresponding to both the maximum power coefficient $C_{p\max}$ and the optimal TSR λ_{opt}, which are of constant values for each wind turbine. The maximum extracted power can be derived from Eq. (1):

$$P_{\max} = K_{opt}\omega_{opt}^3 \quad \text{. . . . .} \quad (4)$$

where

$$K_{opt} = \frac{0.5\pi\rho C_{p\max}R^5}{\lambda_{opt}^3}$$

$$\omega_{opt} = \frac{\lambda_{opt}}{R}v.$$

Thus, in order to extract maximum power, the turbine must always rotate at $\omega_r = \omega_{opt}$. This can be achieved with the TSR control method. Given wind speed information, the TSR control method regulates rotor speed at optimum speed in order to maintain TSR at an optimum value.

3. Proposed Fuzzy Wind Speed Estimator

Input-output mapping problems can be solved in many ways such as using fuzzy systems, linear systems, expert systems, neural networks, differential equations, or interpolated multidimensional look-up tables. Among those ways, the fuzzy system is often the best. It is well known for its convenient use for developing approximate functions in terms of *if-then* rules. The main advantage of using the fuzzy system that other methods do not have is the ease of incorporating the expert knowledge, which is not necessarily precise. This applies to the work in this paper as well.

Fig. 3. Fuzzy wind speed estimator model.

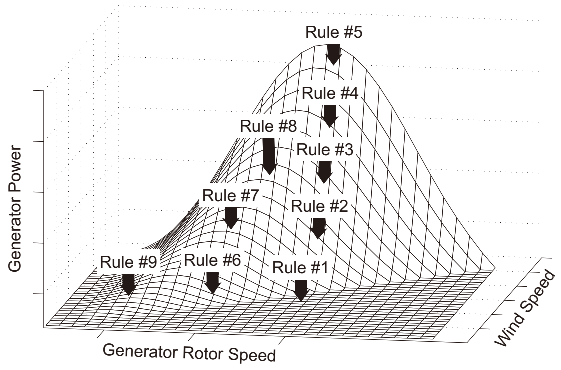

Fig. 4. Points on the power curve where if-then rules are inferred.

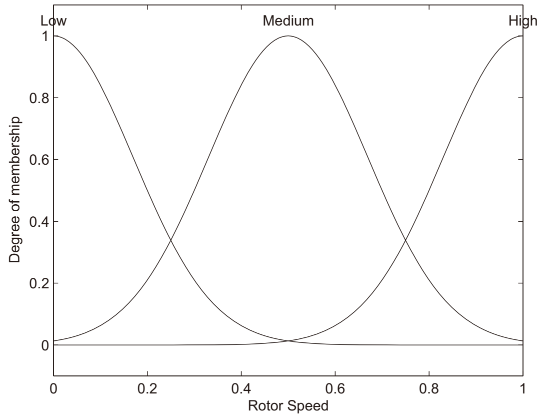

Fig. 5. Membership functions of rotor speed.

The wind speed estimator proposed in this paper is built using a fuzzy system as shown in **Fig. 3**, which is so-called fuzzy wind speed estimator (FWSE). The main idea behind FWSE is to use the fuzzy rules *if-then* which are inferred from a typical power curve without any training or optimization.

The power curve of the wind turbine has a typical form as shown in **Fig. 2**, characterized with three variables: extracted wind power, turbine rotor speed, and wind speed. When the power curve is known, we may be able to determine the wind speed, given information of the extracted power and the turbine rotor speed. In reality, the true power curve is unknown. In addition, all the power curve variables are impractical to measure directly. For convenience in this paper they are replaced by the power and the rotor speed of the generator, except the wind speed, as shown in **Fig. 4**. Each point on the power curve corresponds to a state consisting of the three variables, each of which is a state variable.

Considering that the typical form of the power curve is relatively the same for most of wind turbines, several general fuzzy rules for wind speed estimation can be heuristically inferred from the power curve as shown in **Fig. 4**. The antecedent variables are both the rotor speed and the extracted power. The consequent variable is the wind speed. The way of inferring the fuzzy rules is explained below.

The certain points on the power curve shown by the down arrows in **Fig. 4** are supposed to be the centers of unique clusters. Each unique cluster represents a unique relationship between the state variables in the cluster. Each unique relationship can be stated linguistically using a single fuzzy rule.

Before inferring the effective fuzzy rules based on the locations of the chosen clusters shown in **Fig. 4**, some assumptions are required. The states are assumed to take place in the partial-load regime of WECS in which the extracted power at a given wind speed must depend on the rotor speed. The turbine rotor is assumed not rotating at low speed when subject to high wind speed, which is the case in the WECS control tracking maximum power points under wind speed variation. This means that the states on the left side of the maximum power line are assumed unlikely to take place. On the contrary, the states are desired to mostly take place near to or on the right side of the maximum power line. These assumptions are required to reduce the number of the fuzzy rules required for the wind speed estimation. If the clusters on the left side of the maximum power line were to be chosen as well for defining the fuzzy rules, there would be a redundant number of the fuzzy rules. This is due to somewhat symmetrical form of the power curve, having the different states on the left and the right side of the maximum power line but suggesting the same wind speed.

The fuzzy rules for FWSE are built with fixed numbers of membership functions for both input and output parts. The ranges of both parts are normalized within $[0, 1]$.

Figure 5 shows the membership functions of the generator rotor speed defined using three Gaussian membership functions, each of which is labeled with *low, medium, high*, respectively with the center at 0, 0.5, and 1.

Figure 6 shows the membership functions of the generator power defined using five Gaussian membership functions, each of which is labeled with *zero, low, medium, high, very high* respectively with the center at 0, 0.254, 0.5, 0.773, and 1. The standard deviation for all the membership functions is set to 0.169.

By using the Takagi-Sugeno type [19], the membership functions of the output part of FWSE are simply represented with the constants of 0, 0.25, 0.5, 0.75, and 1, respectively labeled with *very low, low, average, high,* and *very high*.

Let P_g denote the measured generator power, ω_g the

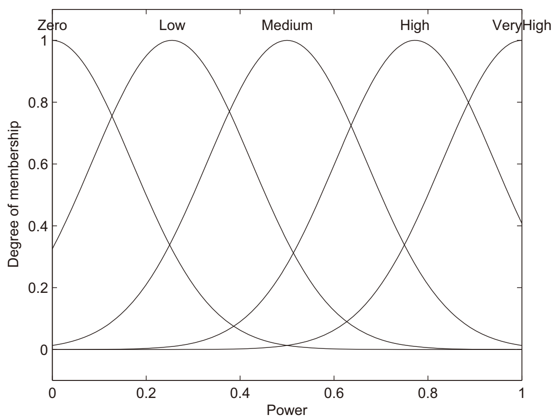

Fig. 6. Membership functions of generator power.

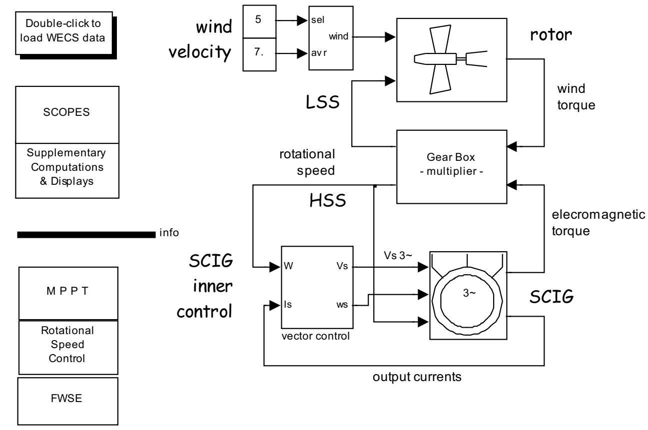

Fig. 7. SCIG-based WECS model.

generator rotor speed, and $\hat{v}$ the wind speed estimate. The fuzzy rules to be used in FWSE, which are inferred from the chosen points on the power curve as shown in **Fig. 4**, can be stated as follows:

1. if ω_g is *high* and P_g is *zero* then $\hat{v}$ is *very low*
2. if ω_g is *high* and P_g is *low* then $\hat{v}$ is *low*
3. if ω_g is *high* and P_g is *medium* then $\hat{v}$ is *average*
4. if ω_g is *high* and P_g is *high* then $\hat{v}$ is *high*
5. if ω_g is *high* and P_g is *very high* then $\hat{v}$ is *very high*
6. if ω_g is *medium* and P_g is *zero* then $\hat{v}$ is *very low*
7. if ω_g is *medium* and P_g is *low* then $\hat{v}$ is *low*
8. if ω_g is *medium* and P_g is *medium* then $\hat{v}$ is *average*
9. if ω_g is *low* and P_g is *zero* then $\hat{v}$ is *very low*.

Normalized input and output parts of the fuzzy rules make the rules generally applicable to any wind turbine with the same typical power curve. Although different specifications of wind turbines might lead to differences in the operating ranges of the input and output variables of FWSE, the fuzzy structure inside FWSE, either in terms of its fuzzy rules or its membership functions, does not necessarily change when given different specification of wind turbine.

4. Case Study

In this section the WECS model used, the wind speed generator, and the simulation of the wind speed estimation are discussed. The effectiveness of the proposed FWSE in estimating the wind speed during the WECS operation is elaborated.

4.1. WECS Model

The wind speed estimation was simulated during the operation of the Simulink SCIG-based WECS model as shown in **Fig. 7**, which is a modified version of the original WECS model obtained from [17] (i.e., the file `mppt1.mdl` inside the case study 2). The WECS model

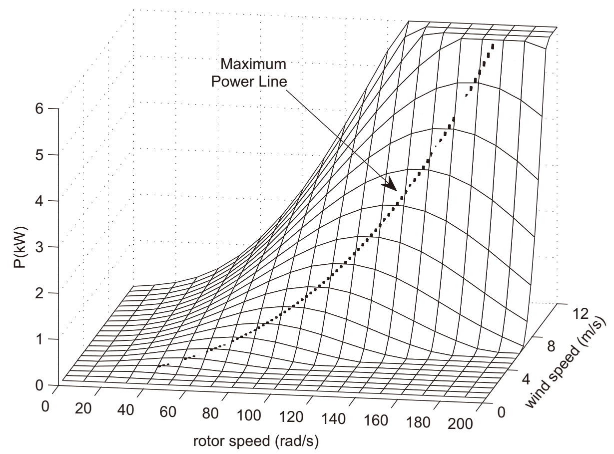

Fig. 8. Power curve of SCIG-based WECS.

behaves according to the power curve shown in **Fig. 8**. The WECS implementation comprises the wind turbine, the induction machine (i.e., SCIG), and the generator-side inverter. The interaction between the electrical grid and WECS is assumed fixed. The electrical grid is taken as ideal because the grid interface is not of interest in the simulation.

The WECS model in **Fig. 7** is limited to operate in the partial-load regime (i.e., under the rated wind speed) and works with the following parameters: the air density $\rho = 1.25$ kg/m^3, the turbine radius $R = 2.5$ m, the optimal tip speed ratio $\lambda_{opt} = 7$, the maximum power coefficient $C_{p\max} = 0.47$, and the multiplier ratio of the gearbox 6.25. With the rated power of 6 kW, the generator rotor speed may vary between 0 until 160 rad/s and the wind speed is less than 12 m/s.

The modified parts of the WECS model in **Fig. 7** are inside the block MPPT and a new block FWSE. Inside the block MPPT we add an implementation of the TSR control, as shown in **Fig. 9**, where the generator rotor speed reference is set proportional to the wind speed. Using the optimum tip speed ratio λ_{opt} and the turbine radius R

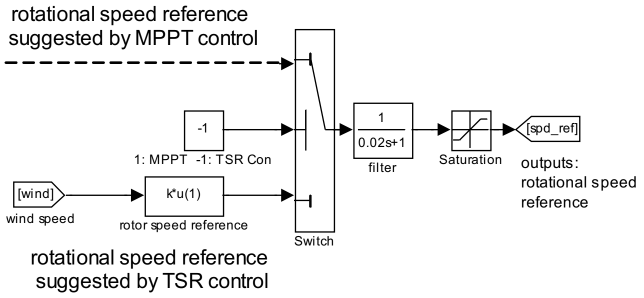

Fig. 9. Added TSR control.

given above, the optimum generator rotor speed reference is

$$\omega_g^* = 6.25\omega_{opt} = k_{opt}v \quad . \; . \; . \; . \; . \; . \; . \; . \; . \quad (5)$$

where

$$k_{opt} = \left(6.25\frac{\lambda_{opt}}{R}\right) = 17.5.$$

In this paper λ_{opt} is assumed unknown, and therefore, the optimum generator rotor speed reference ω_g^* as well. Alternatively, we can use the practical method of estimating k_{opt} proposed in [5]. Once the estimated k_{opt} is obtained, although inaccurate, we may set the generator rotor speed reference by $\omega_g = kv$, where the constant k is any number around the estimated k_{opt}. In this paper, the estimated k_{opt} is assumed available already, but deviates from the true k_{opt}. It will be shown later that the small deviations of k from $k_{opt} = 17.5$ do not lead to significant errors of the wind speed estimation.

The detailed new block FWSE is shown in **Fig. 10** where the operating ranges of the input and output variables are set according to the specification of WECS given above. In the block FWSE the generator rotor speed is limited to be within the range of $[0,160]$ rad/s, the generator power to be within the range of $[0,6000]$ W, and the wind speed to be within $[5,12]$ m/s.

The block FWSE in **Fig. 10** implements a fuzzy inference system (FIS) of a Takagi-Sugeno type. FIS is built using the fuzzy rules *if-then* as defined in Section 3. The input and output variables of FIS are normalized within the range $[0,1]$. The generated power has a negative sign in the WECS model. Its value is reversed before applied to FIS.

There have been many methods proposed for solving the wind speed estimation problem in WECS [1–3, 7, 12–15]. In this paper we are not primarily interested in solving the problem of the wind speed estimation in WECS using FWSE. Instead, we apply a very easy and simple setting for FWSE as if the form of the power curve was symmetrical, while other methods offer more complex designs with more difficult setting for the wind speed estimator.

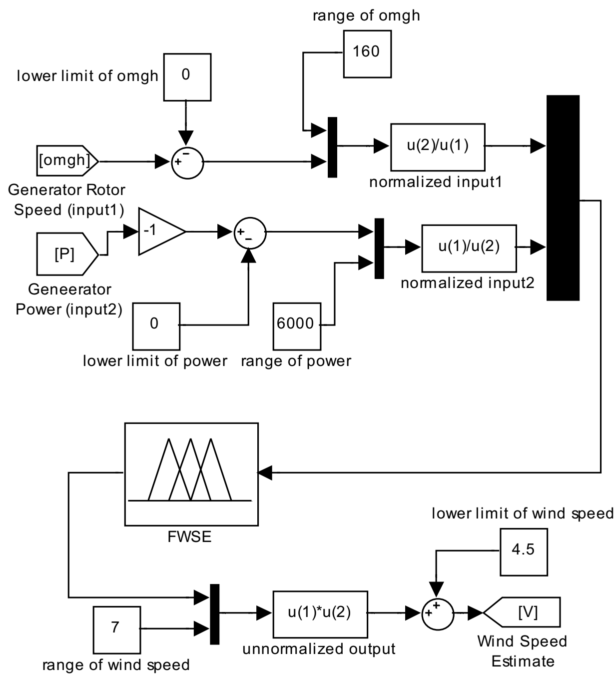

Fig. 10. Simulink model of FWSE.

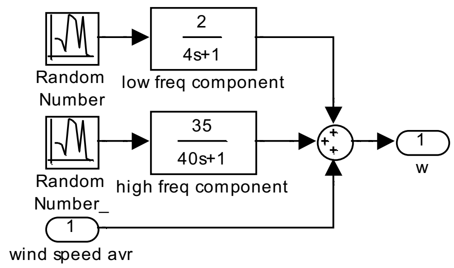

Fig. 11. Wind speed generator.

4.2. Wind Speed Generator

The wind speed profile used in the simulation is generated by the wind speed generator shown in **Fig. 11**. The wind speed average is set to 7 m/s. The wind speed profile should mimic the real one as its generation is based on a non-stationary random process superposing two components: the low-frequency component (i.e., describing long-term and low-frequency variations) and the turbulence component, corresponding to short-term and high-frequency variations. Both frequency components meet the Van der Hoven's wind speed spectral model [18] that represents the real wind speed spectral model.

4.3. Simulation and Results

The wind speed estimation was simulated in six different cases of the control method of WECS and the modified FWSE. In the first case, WECS was controlled by the classical MPPT method. In the second case, WECS was

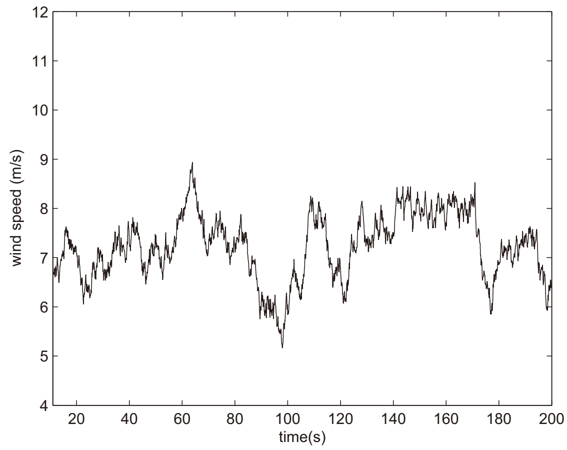

Fig. 12. Wind speed profile.

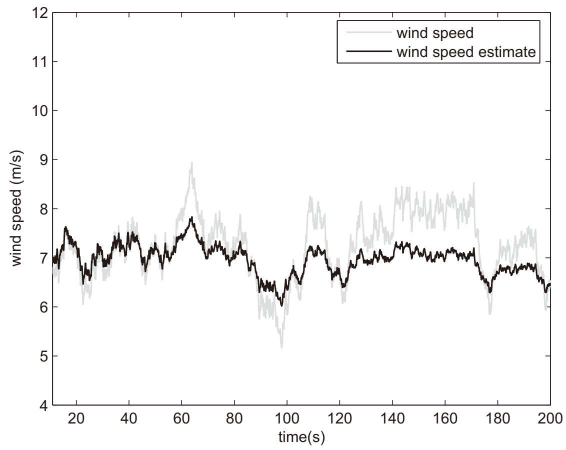

Fig. 13. Wind speed estimate on WECS with MPPT control.

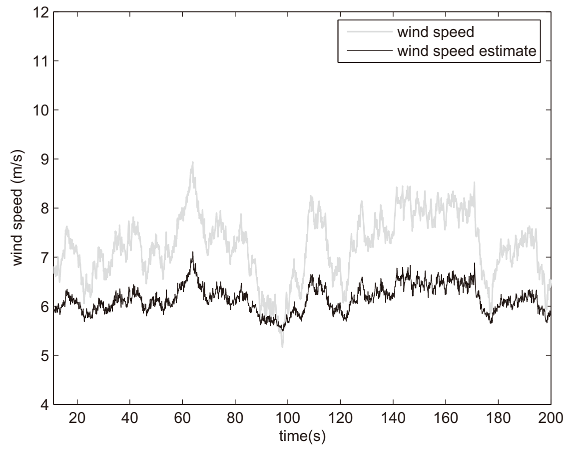

Fig. 14. Wind speed estimate on WECS with TSR control ($k = 10$).

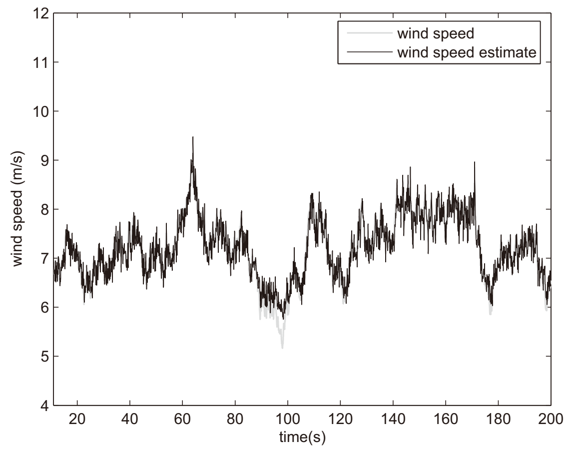

Fig. 15. Wind speed estimate on WECS with TSR control ($k = 18$).

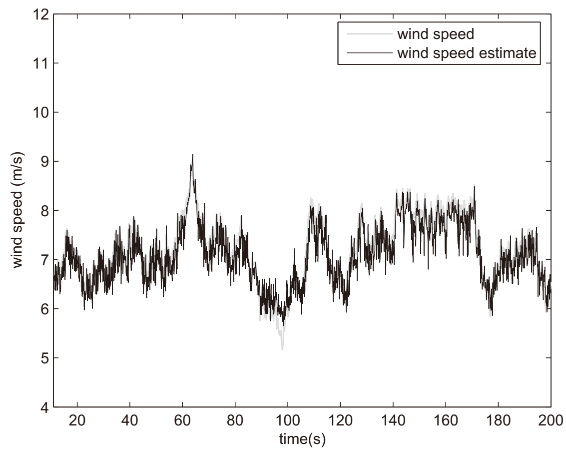

Fig. 16. Wind speed estimate on WECS with TSR control ($k = 20$).

controlled by the TSR method using three different rotor speed references, i.e., $\omega_g = kv$ with $k = 10$, $k = 18$, and $k = 20$. In the third case, WECS controlled by the TSR method but the wind speed estimate $\hat{v}$, instead the original wind speed v, was used to compute the generator rotor speed reference by $\omega_g = k\hat{v}$. The forth case was similar to the third case, except that the wind speed was estimated using FWSE with modified fuzzy rules. The fifth case was also similar to third case, except that the wind speed was estimated using FWSE built with no initial fuzzy rules, but FWSE was optimized by the adaptive neuro fuzzy inference system (ANFIS) method. In the last case the wind speed was estimated using the proposed FWSE optimized with the standard gradient descent method. In all the cases, WECS was operated for 200 s, subject to the wind speed profile shown in **Fig. 12** generated by the wind speed generator in **Fig. 11**.

The results of the wind speed estimation on WECS controlled with the MPPT method and the TSR method using $k = 10$, 18, and 20 are respectively shown in **Figs. 13–16**. Each control method started working after WECS has reached a "normal" operating point, i.e., about 10 s. For this reason, all those simulation results of the wind speed estimation are shown after 10 s.

The wind speed estimates were poor when WECS was controlled using the MPPT method and the TSR method using $k = 10$. Whereas, much better wind speed esti-

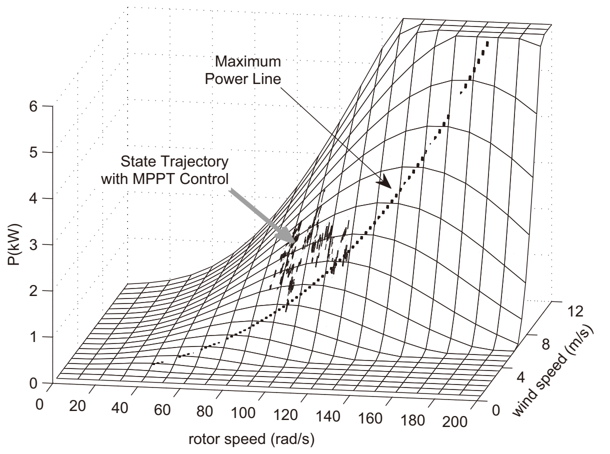

Fig. 17. State trajectory with MPPT control.

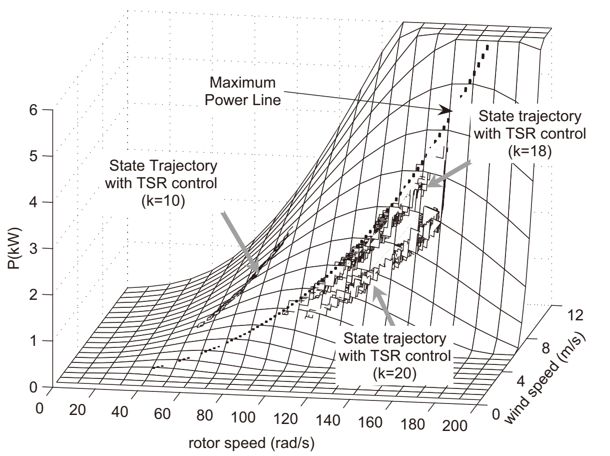

Fig. 18. State trajectory with TSR control.

mates were obtained when WECS was controlled with the TSR method using $k = 18$ (see **Fig. 15**) and $k = 20$ (see **Fig. 16**). The wind speed estimates shown in **Figs. 15** and **16** are very close to the "true" wind speed. Some errors occurred at around the time 100 s at which the wind speed was very near to the lower limit of the output range of FWSE.

Those simulation results can be well understood by looking through the state trajectories on the power curve during the WECS operation for each case. The state trajectory for the case of WECS controlled with the MPPT method is shown in **Fig. 17** and that for the case of WECS controlled with the TSR method is shown in **Fig. 18**. There were about 27 thousands states for the simulation duration of 200 s. The state trajectories shown in both figures were created for every 25 states. As can be seen in both figures, the state trajectories of WECS controlled the MPPT method and the TSR method using $k = 10$ were on left side of the maximum power line. Given such trajectories, the wind speed estimates were poor. Whereas, WECS controlled with the TSR method using $k = 18$ and $k = 20$ resulted in the state trajectories on the right side of the maximum power line and enabled FWSE to much better estimate the wind speed.

The simulation results imply that the locations of the states on the power curve greatly affected the accuracy of the estimation results of the wind speed. They were due to the fuzzy rules in use not representing the entire behavior of the power curve. As illustrated in **Fig. 4**, the proposed fuzzy rules were inferred from the clusters on the right side of the maximum power line. They could well estimate the wind speed when given the states on the right side of or near to the maximum power line. Hence, the maximum power line can be considered as playing a role of a boundary line separating between the states of the right area at which FWSE can well estimate the wind speed and those of the left area at which FWSE will result in poor estimation of the wind speed.

Given the specification of WECS as aforementioned, the maximum power line can be achieved by setting $k = k_{opt} = 17.5$ in the TSR control. The use of any constant k less than 17.5 will result in the states on the left side of the maximum power line, and hence, FWSE will give poor wind speed estimation; otherwise, the states on the right side of the maximum power line will take place, and therefore, lead to better estimation of the wind speed by FWSE.

Unlike the TSR method, the MPPT method uses a random mechanism to achieve optimum states. It perturbs turbine speed, observes a change in power, and then, regulates the turbine speed accordingly to achieve the peak power. It takes many trials-and-errors under wind speed variation and noisy measurement data, resulting in the states randomly distributed on the left or the right side of the maximum power line. Hence, the MPPT method tends to lead to poor performance of FWSE. This drawback may be handled by always regulating the turbine speed high enough before perturbing it and observing a change in power. This approach may be less practical but increase the chances of the states to be on the right side of the maximum power line.

All the above simulations has not demonstrated the case where the TSR control uses the wind speed estimate, instead of the "true" wind speed, to compute the generator speed reference. **Figs. 19** and **20** show the simulation results of the wind speed estimation for the case where the TSR control used the wind speed estimates provided by FWSE to compute the generator rotor speed references. Both figures correspond to the cases of respectively $k = 18$ and $k = 20$. The state trajectories corresponding to both cases are shown in **Fig. 21**. Most of the states were on the right side of the maximum power line. Some states were on the left side of but near to the maximum power line. As expected, given such states, FWSE could well estimate the wind speed.

In addition, the obtained wind speed estimates shown in **Figs. 19** and **20** were smoother than those in **Figs. 15** and **16**. They were different due to the difference in the way of determining the generator rotor speed references. When the generator rotor speed reference is determined using

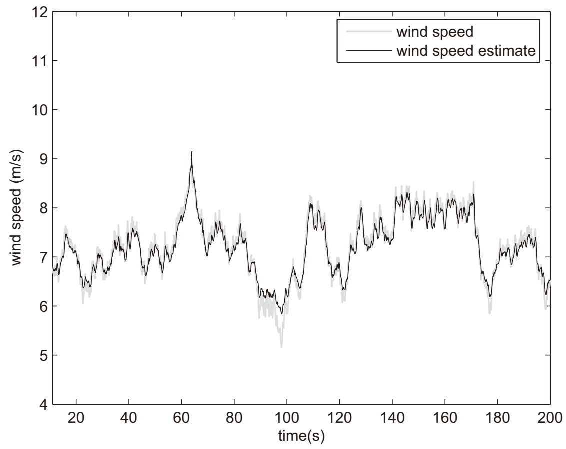

Fig. 19. Wind speed estimates on WECS with TSR control ($k = 18$) using wind speed estimate.

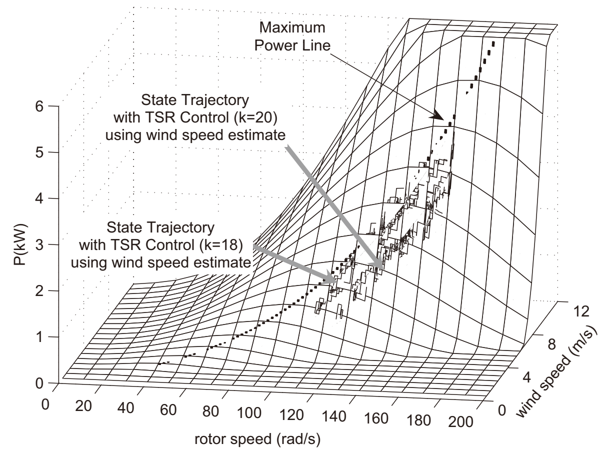

Fig. 21. State trajectory with TSR control using wind speed estimate.

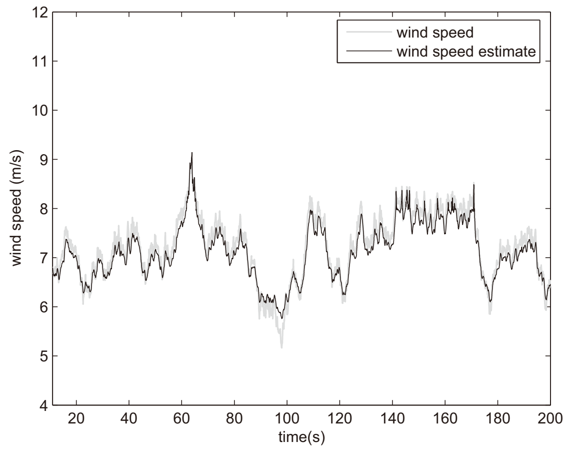

Fig. 20. Wind speed estimates on WECS with TSR control ($k = 20$) using wind speed estimate.

the wind speed estimate in the TSR control, the wind speed estimation takes places in a closed loop involving the TSR controller, WECS, and FWSE. Given an initial state of WECS, FWSE estimates the wind speed. The wind speed estimate is then used by the TSR controller to determine the speed reference at which the generator rotor must rotate. The TSR control applies the low pass filtering process on the generator rotor speed reference before really using it as the final rotor speed reference (see **Fig. 9**). WECS then generates the power and a new state takes place. Hence, each wind speed estimate actually depends indirectly on the previous wind speed estimate. Due to the low pass filtering process taking place continuously in the closed loop, smoother wind speed estimates were obtained as shown in **Figs. 19** and **20**.

The above results have demonstrated the main strength of the fuzzy logic principles to solve the wind speed estimation problem in WECS. Generally speaking, the proposed fuzzy rules used in FWSE are of significance but of course lack of precision. They were simply inferred from the imprecise knowledge picked up from the power curve without any training or optimization. The centers and the shapes of the membership functions of the fuzzy rules were imprecisely chosen by ignoring the fact that the form of the power curve is asymmetrical. The centers of the membership functions were assigned with just equally-spaced constants, regardless of their appropriateness. The most suitable shapes of the membership functions to choose were considered as unknown. Therefore, we can not expect that FWSE would result in highly accurate estimation of the wind speed. Despite applying such a very easy, simple, and imprecise setting, FWSE could achieve good performance with the estimation errors less than 0.5 m/s, comparable with other approaches in [10, 11] giving the estimation errors of up to about 0.5 m/s.

In order to validate the proposed FWSE as a fuzzy model, FWSE using different numbers of the fuzzy rules and modified parameters of the membership functions was simulated. In the following discussion, we call FWSE/MR1 for FWSE using 4 fuzzy rules, FWSE/MR2 for FWSE using complete fuzzy rules, and FWSE/MP for FWSE using modified parameters of the membership functions.

In FWSE/MR1, only the rule numbers 5, 7, 8, and 9 in the proposed fuzzy rules were used. Those fuzzy rules correspond to the clusters along the maximum power line of the power curve shown in **Fig. 4**.

In FWSE/MR2, beside using nine proposed fuzzy rules, the following fuzzy rules were also used:

1. if ω_g is *medium* and P_g is *high* then $\hat{v}$ is *high*
2. if ω_g is *medium* and P_g is *very high* then $\hat{v}$ is *very high*
3. if ω_g is *low* and P_g is *low* then $\hat{v}$ is *low*
4. if ω_g is *low* and P_g is *medium* then $\hat{v}$ is *average*
5. if ω_g is *low* and P_g is *high* then $\hat{v}$ is *high*
6. if ω_g is *low* and P_g is *very high* then $\hat{v}$ is *very high*.

With those additional fuzzy rules, FWSE/MR2 included

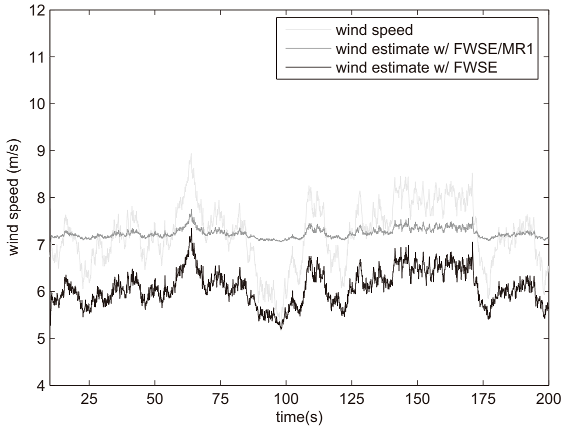

Fig. 22. FWSE/MR1's performance for $k = 10$.

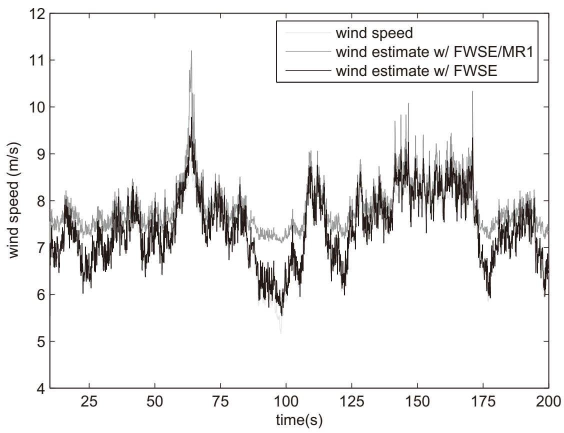

Fig. 23. FWSE/MR1's performance for $k = 18$.

all possible fuzzy rules defined from all the combinations of the membership functions of both input variables.

In FWSE/MP the centers of the Gaussian membership functions of the generator power were changed to 0, 0.45, 0.65, 0.85, and 1.0 and those of the generator rotor speed to 0, 0.65, and 1.0. The standard deviations of all the Gaussian membership functions were unchanged. The constants of the membership functions of the output part of FWSE were modified to be 0.0, 0.35, 0.65, 0.85, and 1.0. With all those modifications, the centers of the membership functions of the input and the output parts of FWSE were no longer assigned with just equally-spaced constants. They were made more dense as they get closer to the maximum value (i.e., 1.0). Such a heuristic setting was chosen to compromise with the typical form of the power curve where the generator power exponentially increases with both the wind speed and the rotor speed.

The comparison of the performance of FWSE and FWSE/MR1 is shown in **Figs. 22–24** and that of FWSE and FWSE/MR2 in **Figs. 25–27**, respectively for $k = 10$, 18, and 20.

For $k = 10$ the state trajectories were not along the maximum power line of the power curve, and as expected, they lead to worse performance of FWSE/MR1.

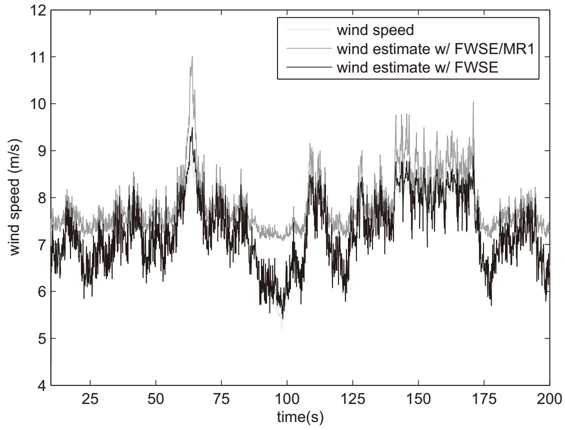

Fig. 24. FWSE/MR1's performance for $k = 20$.

For $k = 18$ and $k = 20$ the state trajectories were near to the maximum power line of the power curve, which should enable FWSE/MR1 to achieve the performance close to the FWSE's performance. However, the performance of FWSE/MR1 was always worse than that of FWSE as shown in **Figs. 22–24**. On the other hand, by using all possible fuzzy rules FWSE/MR2 should better estimate the wind speed, given any state trajectory on the power curve. However, the performance of FWSE/MR2 was not better than that of FWSE for all the three values of k as shown in **Figs. 25–27**. Thus, those results validate that FWSE was the most effective model compared with FWSE/MR1 and FWSE/MR2.

Figures 28 and **29** show the performance of FWSE and FWSE/MP where WECS was controlled with the TSR method using the wind speed estimate and $k = 20$. Setting the lower limit of the wind speed estimate to 4.5 m/s resulted in the performance of FWSE/MP worse than that of FWSE as shown in **Fig. 28**. However, the pattern of the wind speed estimates resulting by FWSE/MP was almost the same as that by FWSE, except that the wind speed estimate was always lower than the actual wind speed. After increasing the lower limit of the wind speed estimate to 5.1 m/s, better wind speed estimates were obtained by FWSE/MP as shown in **Fig. 29**. Particularly at about the time 100 s, FWSE/MP succeeded to better estimate the wind speed with smaller errors than FWSE.

Of course, the good performance of FWSE/MP is only for a specific case. Given the different specification of the wind turbine, FWSE/MP will require different setting. However, any modified version of FWSE can always use FWSE as a good initial model to be optimized later to obtain a more appropriate setting as demonstrated in the following results.

In all the cases of the comparison above, the FWSE's performance was compared only with the counterexamples that were not optimized with proper methods. In the following cases, FWSE was compared with an ANFIS based-FWSE (ANFIS-FWSE) and a Gradient-Descent FWSE (GD-FWSE).

Given FWSE as the initial model, the Matlab's ANFIS

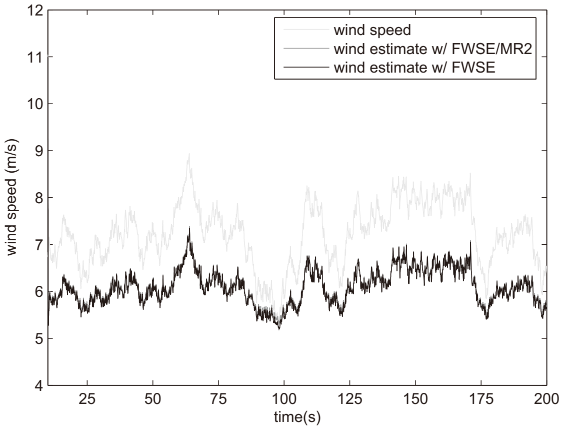

Fig. 25. FWSE/MR2's performance for $k = 10$.

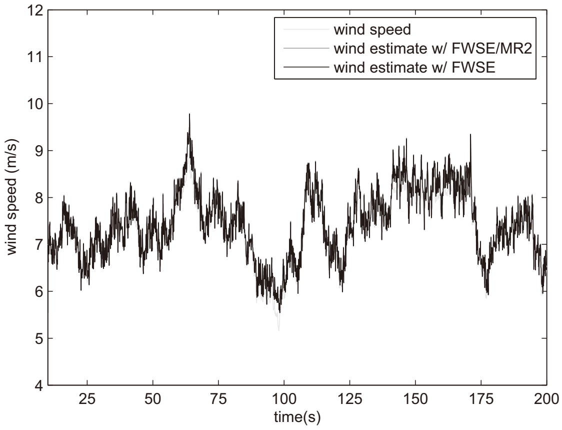

Fig. 26. FWSE/MR2's performance for $k = 18$.

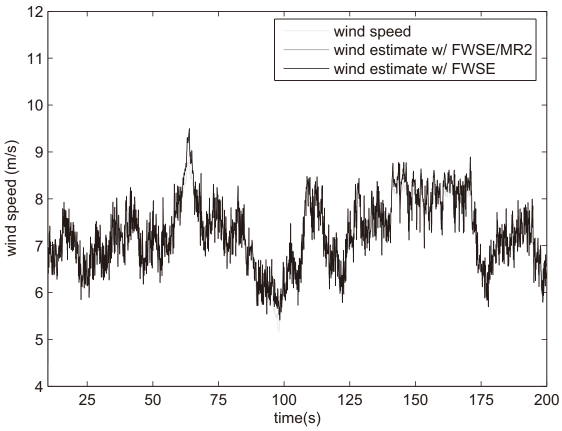

Fig. 27. FWSE/MR2's performance for $k = 20$.

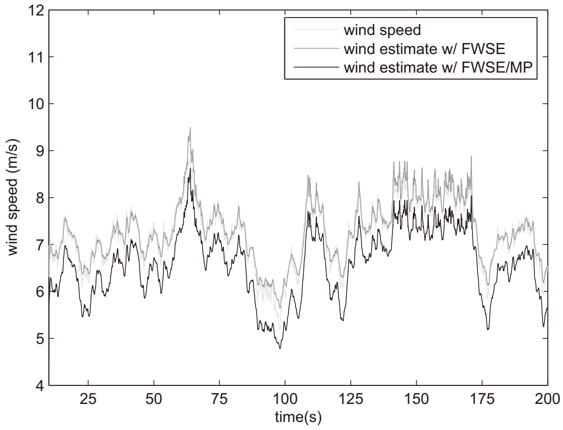

Fig. 28. FWSE/MP's performance with lower limit of wind speed estimate of 4.5 m/s and $k = 20$.

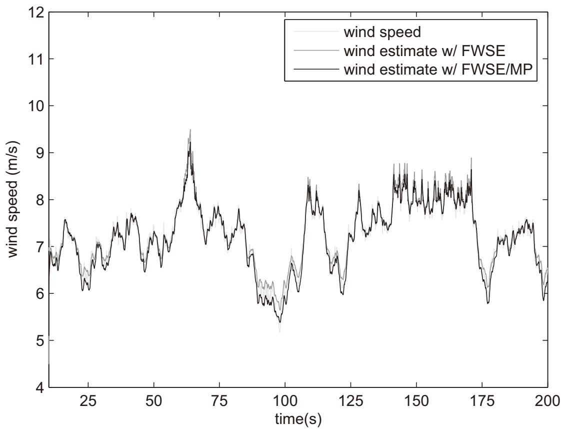

Fig. 29. FWSE/MP's performance with lower limit of wind speed estimate of 5.1 m/s and $k = 20$.

method is expected to produce the best ANFIS-FWSE. Unfortunately, the Matlab's ANFIS method only works when given the maximum number of all possible fuzzy rules. The maximum number of all possible fuzzy rules that can be used in FWSE is 15. Whereas, the number of the proposed fuzzy rules used in FWSE is 9. Therefore, FWSE using the proposed fuzzy rules can not be trained using the Matlab's ANFIS method.

In this paper ANFIS-FWSE was built from scratch. Its input variables, i.e., the generator rotor speed and the generator power, were respectively defined using 3 and 5 equally-spaced Gaussian membership functions. Its output parts were simply 15 constants set to *zero* initially. The fuzzy rules used in ANFIS-FWSE were defined from all possible combinations of both input variables. Both input and output parameters of ANFIS-FWSE were adjusted by the Matlab's ANFIS method in 100 epochs.

The data used for training ANFIS-FWSE were sampled from the typical power curve where the generator rotor speed, the wind speed, and the generator power were respectively limited within the ranges of $[0, 160]$ rad/s, $[0, 12]$ m/s, and $[0, 6]$ kW. Both the generator rotor speed and the wind speed were divided into 60 points and then all their possible combinations were used to compute the corresponding generator power. The power curve used was generated according to the non-dimensional curve C_p versus λ in [17].

GD-FWSE is a trained version of the proposed FWSE. The training was applied after rewriting FWSE in the following compact form [19]:

$$\hat{v} = \Gamma\Theta^T \quad . \quad . \quad . \quad . \quad . \quad . \quad . \quad . \quad . \quad . \quad . \quad . \quad . \quad . \quad . \quad (6)$$

where $\Theta = [\theta_1 \theta_2 \cdots \theta_9]$ is a parameter vector whose elements correspond to the constants of the membership functions of the output part and Γ is a row vector resulting from the implication process in FWSE. The parameters of Γ were not changed during the training. Each element of Θ was adjusted by the following standard gradient-descent update rule:

$$\frac{d\theta}{dt} = -\alpha \frac{\partial Q}{\partial \theta} \quad . \quad . \quad . \quad . \quad . \quad . \quad . \quad . \quad . \quad . \quad . \quad . \quad . \quad (7)$$

where α is a learning rate and Q is the root mean square error (RMSE) defined as

$$Q = \frac{1}{N}\sum_{i}^{N} E_i^2, \quad . \quad . \quad . \quad . \quad . \quad . \quad . \quad . \quad . \quad . \quad . \quad . \quad . \quad (8)$$

where $E_i = v_i - \hat{v}_i$ and N is the data length. GD-FWSE was not trained using the entire data on the power curve, instead only the limited data on the right side of the maximum power line on the power curve.

Some proposed fuzzy rules shared the same output membership functions, i.e., *very low* in the rule numbers 1, 6, and 9; *low* in the rule numbers 2 and 7; and *average* in the rule numbers 3 and 8. Hence, the output parameter vector became

$$\Theta = [\theta_1 \ \theta_2 \ \theta_3 \ \theta_4 \ \theta_5 \ \theta_1 \theta_2 \ \theta_3 \ \theta_1]$$

and the adjustable parameters reduced to only five parameters, i.e., θ_1, θ_2, θ_3, θ_4, and θ_5. However, during the training process, all elements of Θ were adjusted individually using the update rule (7). The latest updates for the first, 6th, and 9th elements of Θ were assigned with an average value of individual updates of the first, 6th, and 9th elements. The latest updates for the second and 7th elements of Θ were assigned with an average value of individual updates of the second and 7th elements. The latest updates for the third and 8th elements of Θ were assigned with an average value of individual updates of the third and 8th elements.

Figure 30 shows the comparison of the wind speed estimate by ANFIS-FWSE, FWSE, and GD-FWSE. Both output and input parameters were adjusted in the training of ANFIS-FWSE. In addition, the output parameters were set to zero initially. This made the training of ANFIS-FWSE take much harder effort to achieve near optimal parameters. Using the root mean square error (RMSE) between the wind speed and its estimate as the performance measure, the performance of FWSE was better than that of ANFIS-FWSE, respectively with RMSE of 0.1158 and 0.2198. The FWSE's performance was satisfactory despite effortless design process. The most important but trivial effort to achieve the good performance of FWSE was to find an appropriate lower limit for the wind speed input variable.

Whereas, after training with the update rule (7), GD-FWSE resulted in the best performance with RMSE of

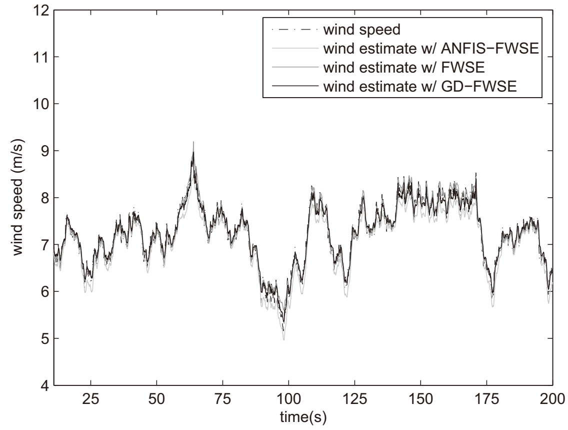

Fig. 30. Wind speed estimation using ANFIS-FWSE and GD-FWSE and $k = 20$.

0.1071. Unlike FWSE, GD-FWSE worked well with full ranges of its variables, i.e., no adjustment of the limits of its input and output variables was required. In addition, its training with only the standard update rule took less effort to achieve near optimal parameters, justifying the effectiveness of the proposed FWSE as a good initial estimator.

5. Conclusion

A power curve based fuzzy wind speed estimator for wind speed estimation in wind energy conversion systems has been presented. It works based on the effective fuzzy rules heuristically inferred from the typical power curve. Nine clusters on the power curve are chosen to represent the behavior of the relationships between the wind speed, the rotor speed, and the extracted power, corresponding to nine fuzzy rules. The performance of the estimator with a very simple, easy, and imprecise setting was simulated for estimating the wind speed during the operation of the SCIG-based wind energy conversion system. The simulation results showed that the fuzzy wind speed estimator could well estimate the changing wind speed.

References:

[1] M. Abdullah, A. Yatim, C. Tan, and R. Saidur, "A review of maximum power point tracking algorithms for wind energy systems," Renewable and Sustainable Energy Reviews, Vol.16, pp. 3220-3227, 2012.

[2] H. Li, K. L. Shi, and P. McLaren, "Neural-network-based sensorless maximum wind energy capture with compensated power coefficient," IEEE Trans. Ind. Appl., Vol.41, Issue 6, pp. 1548-1156, 2005.

[3] A. Mesemanolis and C. Mademlis, "A Neural Network Based MPPT Controller for Variable Speed Wind Energy Conversion Systems," 8th Mediterranean Conf. on Power Generation, Transmission, Distribution and Energy Conversion (MEDPOWER 2012), 2012.

[4] M. Monfared, H. Rastegar, and H. M. Kojabadi, "A new strategy for wind speed forecasting using artificial intelligent methods," Renewable Energy, Vol.34, pp. 845-848, 2009.

[5] A. Naba, A. Nadhir, and T. Hiyama, "Fuzzy model power curve based linear controller for maximum wind energy extraction in vari-

able speed wind energy conversion system," The 2011 IFSA World Congress and the 2011 AFSS, 2011.

[6] A. Nadhir, A. Naba, and T. Hiyama, "FIS/ANFIS Based Optimal Control for Maximum Power Extraction in Variable-speed Wind Energy Conversion System," IEEJ Trans. on Power and Energy, Vol.131, No.8, pp. 708-714, 2011.

[7] A. G. Abo-Khalil and D. C. Lee, "MPPT control of wind generation systems based on estimated wind speed using SVR," IEEE Trans. Ind. Appl., Vol.55, Issue 3, pp. 1489-1490, 2008.

[8] M. Azzouz, A. l. Elshafei, and H. Emara, "Evaluation of fuzzy-based maximum power-tracking in wind energy conversion systems," IET Renewable Power Generation, Vol.5, Issue 6, pp. 422-430, 2011.

[9] R. Rocha, "A sensorless control for a variable speed wind turbine operating at partial load," Renewable Energy, Vol.36, pp. 132-141, 2011.

[10] J. Brahmi, L. Krichen, and A. Ouali, "A comparative study between three sensorless control strategies for PMSG in wind energy conversion system," Applied Energy, Vol.86, Issue 9, pp. 1565-1573, 2009.

[11] M. Pucci and M. Cirrincione, "Neural MPPT Control of Wind Generators With Induction Machines Without Speed Sensors," IEEE Trans. on Industrial Electronics, Vol.58, Issue 1, pp. 37-47, 2011.

[12] W. Qiao, W. Zhou, J. M. Aller, and R. G. Harley, "Wind speed estimation based sensorless output maximization control for a wind turbine driving a dfig," IEEE Trans. on Power Electronics, Vol.23, pp. 1156-1169, 2008.

[13] V. Calderaro, V. Galdi, A. Piccolo, and P. Siano, "A fuzzy controller for maximum energy extraction from variable speed wind power generation systems," Electric Power Systems Research, Vol.78, pp. 1109-1118, 2008.

[14] V. Galdi, A. Piccolo, and P. Siano, "Designing an Adaptive Fuzzy Controller for Maximum Wind Energy Extraction," IEEE Trans. On Energy Conversion, Vol.23, Issue 2, pp. 559-569, 2008.

[15] V. Galdi, A. Piccolo, and P. Siano, "Exploiting maximum energy from variable speed wind power generation systems by using an adaptive Takagi–Sugeno–Kang fuzzy model," Energy Conversion and Management, Vol.50, pp. 413-421, 2009.

[16] A. Naba, "Fuzzy Logic Principles for Wind Speed Estimation in Wind Energy Conversion Systems," Int. Conf. on Information Technology and Electrical Engineering (ICITEE) 2014, 2014.

[17] I. Munteanu, A. I. Bratcu, N. Cutululis, and E. Ceanga, "MATLAB®Case-study Simulations," http://www.springer.com/gp/book/9781848000797 [accessed August 26, 2015]

[18] I. Munteanu, A. I. Bratcu, N.-A. Cutululis, and E. Ceang, "Optimal Control of Wind Energy Systems, Towards a Global Approach," Advances in Industrial Control, Springer-Verlag London Ltd., 2008.

[19] L.-X. Wang, "A course in fuzzy systems and control," Prentice-Hall International, Inc., 1997.

Name:
Agus Naba

Affiliation:
Study Program of Instrumentation, Department of Physics, Faculty of Mathematics and Natural Sciences, University of Brawijaya

Address:
Jl. Veteran, Malang, East Java 65145, Indonesia

Brief Biographical History:
1996- Joined Department of Physics, University of Brawijaya
2007- Ph.D. degree from University of Tsukuba
2010- Visiting Researcher, Kumamoto University
2017- Head of Study Program of Instrumentation, University of Brawijaya

Main Works:
• "Fuzzy Logic Principles for Wind Speed Estimation in Wind Energy Conversion Systems," Int. Conf. on Information Technology and Electrical Engineering (ICITEE) 2014, 2014.

Membership in Academic Societies:
• Indonesian Society of Physics (HFI)

Name:
Ahmad Nadhir

Affiliation:
Study Program of Instrumentation, Department of Physics, Faculty of Mathematics and Natural Sciences, University of Brawijaya

Address:
Jl. Veteran, Malang, East Java 65145, Indonesia

Brief Biographical History:
1999- Joined Department of Physics, University of Brawijaya
2011- Ph.D. degree from Kumamoto University
2015- Secretary of Department of Physics, University of Brawijaya

Main Works:
• "FIS/ANFIS based optimal control for maximum power extraction in variable-speed wind energy conversion system," IEEJ Trans. on Power and Energy, Vol.131, No.8, pp. 708-714, 2011.

Membership in Academic Societies:
• Indonesian Society of Physics (HFI)